# Nonlinear Wave Loading on a Vertical Cylinder in Wave Groups with Diverse Spreading

**Haoyu Ding[1*], Jun Zang[1], Paul H. Taylor[2], Thomas A. A. Adcock[3], Saishuai Dai[4], Dezhi Ning[5], Lifen Chen[5], Jinxuan Li[5]**
[1]Department of Architecture & Civil Engineering, University of Bath, Bath, UK
[2]Oceans Graduate School, The University of Western Australia, Perth, Australia
[3]Department of Engineering Science, University of Oxford, Oxford, UK
[4]Kelvin Hydrodynamics Laboratory, University of Strathclyde, Glasgow, UK
[5]SKLCOE, Dalian University of Technology, Dalian, China
*Email: hd484@bath.ac.uk

## 1 INTRODUCTION

Accurately predicting nonlinear wave loading is essential for the safe and efficient design of marine and offshore structures. However, this task remains complex due to the inherent challenges of capturing wave-structure interactions under extreme conditions. Previous studies have predominantly focused on uni-directional extreme waves and their impact on vertical cylinders, where significantly nonlinear forces are observed [1]. This study extends the investigation to multi- and bi-directional wave group interactions with vertical cylinders. By comparing nonlinear wave loads across various wave spreading types, we highlight the commonalities and differences in wave-induced forces across diverse spreading-type wave conditions. The analysis incorporates Stokes-type force harmonics, derived using the phase-based harmonic separation method [1], and the shorter duration quasi-impulsive forces and secondary load cycles that contribute to a cylinder's ringing response [2].

## 2 WAVE CONDITIONS

This research was conducted experimentally as a part of the UK-funded EPSRC Sea-Swallows project. The study used focused wave groups generated based on NewWave theory, representing short-term severe wave conditions. The target focus point of these waves was positioned at the centre of a vertical cylinder. A JONSWAP spectral form was used to generate the wave groups. Local wave group properties at the focus point were first measured in an empty tank (i.e., without the cylinder), and the same groups were later used in tests involving the cylinder interaction.

In addition to uni-directional waves, the study examined bi-directional waves, which consisted of two crossing wave groups with identical wave amplitudes and peak periods intersecting at the focus point. The crossing angles ($\theta$) between the two wave groups were set to 20° and 40°, with each wave at ±10° and ±20° relative to the normal off the wave paddles, respectively. For multi-directional waves, the Mitsuyasu-type spreading function $\cos^{2s}(\theta/2)$ [3] was employed. The root-mean-square angle ($\sigma$) was set to approximately 20° and 30°, corresponding to $s$ = 15 and 7.

Various wave spreading patterns were successfully generated in the lab, as shown in Fig 1. At the focus point, multi-directional waves formed a hyperbolic pattern, while bi-directional waves created an X-shaped pattern. The time histories of free-surface elevation at the focus point are also illustrated in Fig 1.

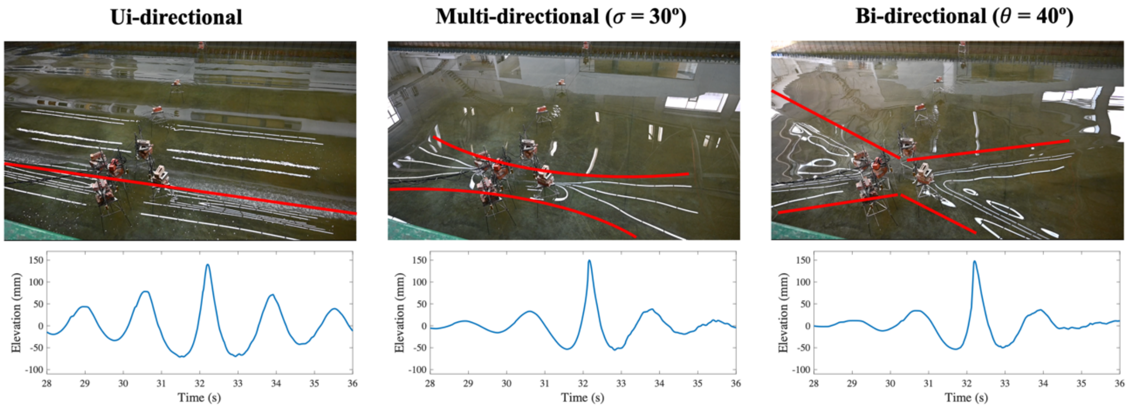


Figure 1: Wave spreading patterns in an empty wave tank and free surface elevation time histories at the focus location under various wave conditions: uni-directional wave ($T = 1.64$ s, $A_L = 0.10$ m); multi-directional wave ($T = 1.64$ s, $A_L = 0.10$ m, $\sigma = 30°$); bi-directional wave ($T = 1.64$ s, $A_L = 0.10$ m, $\theta = 40°$).

## 3 RESULTS

This section discusses Stokes-type force harmonics, impulsive forces, and secondary load cycles, analysing specific wave conditions as example cases. Additional results, including computational fluid dynamics (CFD) simulations, will be presented at the workshop.

### 3.1 Stokes-Type Nonlinear Forces

A phase decomposition method [1] is employed to cleanly separate Stokes-type nonlinear force components. Previous work [4] demonstrated that this method is also applicable to directionally spreading waves, as confirmed by the new experimental results.

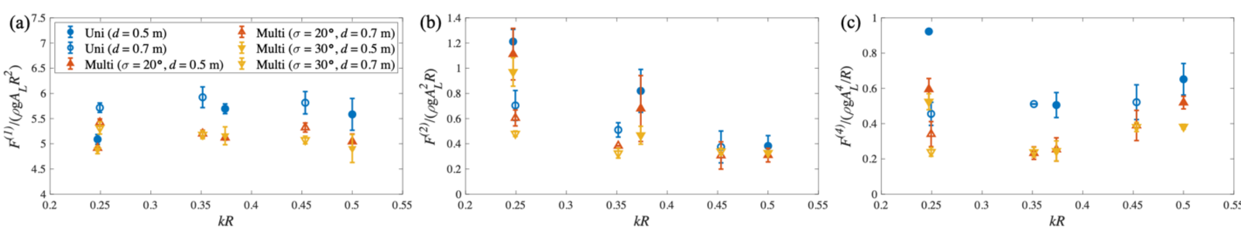


Figure 2: Non-dimensional (a) linear, (b) 2nd- and (c) 4th-order force harmonics for uni- and multi-directional waves as a function of $kR$ ($k$ is the wave number and $R$ is the cylinder radius), where $F^{(n)}$ refers to the $n$th-order harmonic force in frequency.

Using the phase decomposition method, Figure 2 presents normalised linear, 2nd-, and 4th-order force harmonics, calculating the mean values of the non-dimensional force harmonics for a group of wave cases with the same peak wave period but varying wave amplitudes. The trend of the force harmonics aligns well with findings from [1]. Multi-directional wave cases are compared with uni-directional wave cases, consistently showing smaller harmonic values. As the root-mean-square (RMS) spreading angle ($\sigma$) is increased, the harmonic values decrease, and the differences become more pronounced for higher-order harmonics. Notably, the 4th-order force harmonics in multi-directional waves are significantly smaller than those in uni-directional waves.

Fig 3 examines the relationship between uni-directional and multi-directional wave force harmonics ($\sigma = 20°$). The peak values of the $n$th-frequency force harmonics for multi-directional waves, when multiplied by the coefficient $1/\cos^n(\sigma)$, closely match the corresponding peak values for uni-directional waves. This relationship shows good agreement for the linear and 4$^{th}$-order harmonics, and slightly worse for the 2$^{nd}$-order harmonics, likely due to differing spectral enhancement factors.

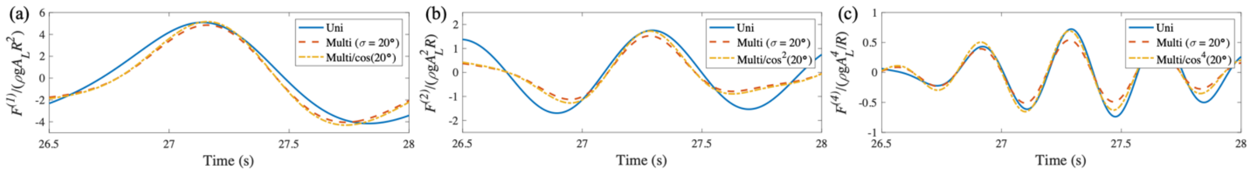


Figure 3: (a) Linear, (b) 2$^{nd}$-, and (c) 4$^{th}$-order force harmonics for uni- and multi-directional waves ($T$ = 1.64 s, $A_L$ = 0.10 m, $d$ = 0.5 m), with results scaled from multi-directional wave data x $1/cos^n(\sigma)$.

### 3.2 Impulsive Force and Secondary Load Cycle

In addition to Stokes-type nonlinear forces, this section examines wave impact and secondary load cycles for different wave spreading types.

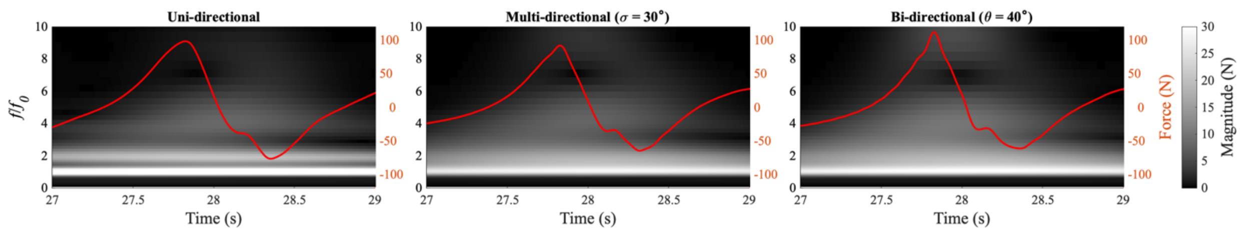


Figure 4: Wavelet analysis of total wave forces for uni-, bi- and multi-directional waves ($T$ = 1.64 s, $A_L$ = 0.10 m, $d$ = 0.5 m) over frequency (normalised by the peak incoming wave frequency, $f_0$) and time.

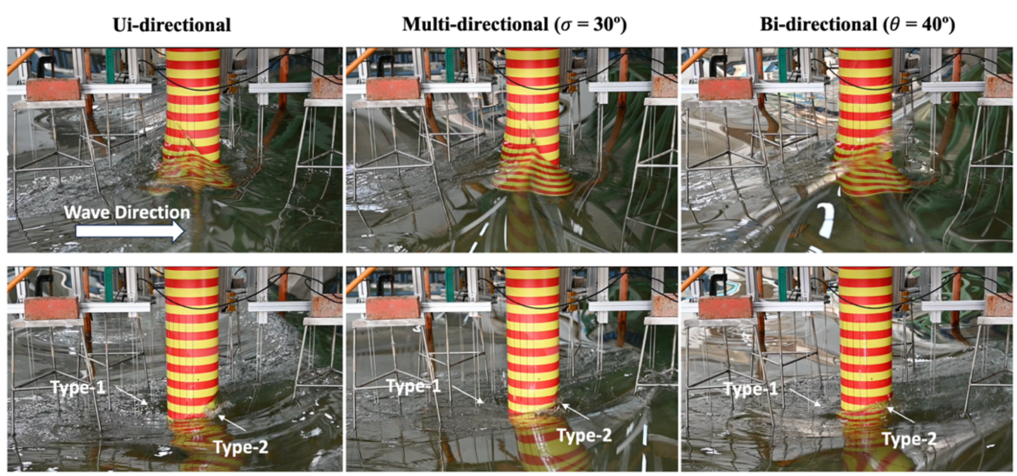


Figure 5: Snapshots from the side view of the cylinder at the time points of (top panel) wave impact and (bottom panel) type-1 and type-2 waves associated with the secondary load cycle.

Fig 4 compares total wave forces as a function of frequency and time for waves with the same peak period and linearised amplitude. Despite differences in spreading types, the wave force time histories exhibit similar values and patterns. Around 27.7 sec, all wave forces show oscillations associated with secondary load cycles, with nonlinear components occurring at higher frequencies (lighter colour at $f/f_0 \sim 3$ to 5). While uni- and multi-directional waves have comparable peak crest values, bi-directional waves exhibit an earlier additional spike at ~ 27.25 sec, resulting from a small slam contribution and giving a slightly higher peak force, with elements beyond $f/f_0 = 8$.

Fig 5 provides side-view snapshots of the cylinder at two critical time points. The top panel captures wave impact on the cylinder's front on the left, where significant wave run-up occurs for uni- and multi-directional waves. Bi-directional waves break at the cylinder's front, causing the force spike seen in Fig 4. The bottom panel shows consistent wave patterns across all cases, with Type-1 and Type-2 waves, as described in [5], associated with secondary load cycles. Point pressures at 0.10 m below the still water level are shown in Fig 6. While discrepancies are observed at the troughs of the pressure-time curves, the local distributions of pressure oscillations caused by scattered waves remain generally consistent. These similarities correspond to the wave field patterns depicted in Fig 5.

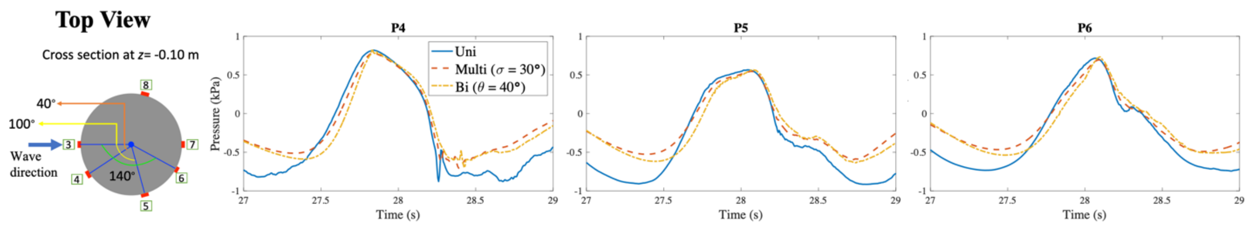


Figure 6: Point pressures measured on the cylinder at 0.10 m below the still water level ($z$ = -0.10 m).

## 4 CONCLUSIONS

The relationship between uni-directional and multi-directional wave-induced force harmonics in frequency has been examined. Directional spreading always appears to lead to relatively smaller high-frequency nonlinear forces in otherwise comparable wave fields. Roughly and empirically, the multi-directional frequency harmonics are reduced by a simple factor ~ $\cos^n(\sigma)$ compared to those in an otherwise similar uni-directional wave, where $\sigma$ is the RMS wave spreading angle and $n$ is the harmonic number in frequency. We also observe that bi-directional and multi-directional waves induce secondary load cycles and short wave scattering similar to uni-directional waves.

## REFERENCES


[1] Chen, L., Zang, J., Taylor, P. H., Sun, L., Morgan, G., Grice, J., Orszaghova, J., Ruiz, M. T., 2018. *An experimental decomposition of nonlinear forces on a surface-piercing column: Stokes-type expansions of the force harmonics*. J. Fluid Mech., 848, 42–77.

[2] Grue, J., Huseby, M., 2002. *Higher-harmonic wave forces and ringing of vertical cylinders*. Appl. Ocean Res., 24(4), 203-214.

[3] Longuet-Higgins, M. S., Cartwright, D. E., Smith, N. D., 1963. *Observations of the directional spectrum of sea waves using the motions of floating buoy*. *Ocean Wave Spectra*. Prentice-Hall Inc., Englewood Cliffs, NJ, 111-136

[4] Ding, H., Zhao, G., Tang, T., Taylor, P. H., Adcock, T. A. A., Dai, S., Ning, D., Chen, L., Li, J., Wang, R., Zang, J., 2025. *Experimental Investigation of Nonlinear Forces on a Monopile Offshore Wind Turbine Foundation Under Directionally Spread Waves.* ASME. J. Offshore Mech. Arctic Eng., 147(4), 042002.

[5] Ding, H., Zang, J., Tang, T., Taylor, P. H., Adcock, T. A. A., Zhao, G., Dai, S., 2024. *An investigation of high-order harmonics in the pressure field around a vertical cylinder in steep wave conditions*. IWWWFB, 14-17 April 2024, St Andrews, Scotland.